Korean J. Chem. Eng., **21**(2), 537-547 (2004)

A Comparative Theoretical Study of Au, Ag and Cu Adsorption on TiO_2 (110) Rutile Surfaces

Devina Pillay, Yun Wang and Gyeong S. Hwang†

Department of Chemical Engineering and Institute of Theoretical Chemistry,
The University of Texas at Austin, Austin, Texas 78712, USA
(*Received 16 October 2003 • accepted 29 December 2003*)

Abstract−The adsorption properties of Au, Ag and Cu on TiO_2 (110) rutile surfaces are examined using density functional theory slab calculations within the generalized gradient approximation. We consider five and four different adsorption sites for the metal adsorption on the stoichiometric and reduced surfaces, respectively. The metal-oxide bonding mechanism and the reactivity of metal atoms are also discussed based on the analyses of local density of states and charge density differences. This study predicts that Au atoms prefer to adsorb at the fourfold hollow site over the fivefold-coordinated Ti(5c) and in-plane and bridging O(2c) atoms with the adsorption energy of ≈0.6 eV. At this site, it appears that the covalent and ionic interactions with the Ti(5c) and the O(2c), respectively, contribute synergistically to the Au adsorption. At a neutral F_s^0 center on the reduced surface, Au binds to the surface via a rather strong ionic interaction with surrounding sixfold-coordinated Ti(6c) atoms, and its binding energy is much larger than to the stoichiometric surface. On the other hand, Ag and Cu strongly interact with the surface bridging O(2c) atoms, and the site between two bridging O(2c) atoms is predicted to be energetically the most favorable adsorption site. The adsorption energies of Ag and Cu at the B site are estimated to be ≈1.2 eV and ≈1.8 eV, respectively. Unlike Au, the interaction of Ag and Cu with a vacancy defect is much weaker than with the stoichiometric surface.

Key words: Gold, Silver, Copper, Titania, Adsorption, Density Functional Theory, Slab Calculation

INTRODUCTION

The synthesis and characterization of "so-called" nanoparticles with the size of 1-10 nm has become a major interdisciplinary area of research over the last decade. These particles have distinctly different electrical, optical, mechanical, and chemical properties from their corresponding bulk solid. Particularly, nanometer sized noble metal particles dispersed on TiO_2 or other oxides have been found to exhibit high catalytic activities [Bell, 2003; Santra and Goodman, 2002]. Au has long been known to be chemically inert in its bulk form, as compared to other transition metals [3], such that it has received little attention as a catalyst. However, TiO_2 supported Au nanoparticles show an extraordinarily high activity for low-temperature catalytic combustion, partial oxidation of hydrocarbons, hydrogenation of unsaturated hydrocarbons, and reduction of nitrogen oxides [Haruta, 1997]. The catalytic properties appear to be very sensitive to the size of Au particles, and that only particles in the range of 2-3 nm are very active [Valden et al., 1998]. Similarly, TiO_2-supported small Ag particles (2-4 nm) also exhibit high catalytic activity and selectivity for propylene epoxidation and low-temperature CO oxidation [de Oliveira et al., 2001], (while larger Ag clusters are much less active [Hayash et al., 1998]). These observations have led to a speculation that there may exist a range of critical particle sizes at which all metals exhibit unusual catalytic properties [Choudhary and Goodman, 2002].

Due to weak metal-support interfacial interactions, however, the small metal particles are easily rearranged and become unstable toward sintering in response to changes in the gaseous environment even at moderate temperatures [Kolmakov and Goodman, 2000, 2001; Campbell et al., 2002]. This may lead to the loss of their catalytic activity, which is indeed a serious problem of oxide supported nanometal catalysts. A comprehensive description of such structural changes is therefore strongly necessary to better understand the underlying mechanism and performance of supported metal catalysts in realistic operation conditions.

The growth of metal particles and their structural changes are a strong function of the surface structure of an oxide support, the elementary processes of metal atoms (such as adsorption, diffusion, and agglomeration) on the surface, and the interfacial interactions of metal particles with an oxide support. The metal-oxide interfacial interactions would also play an important role in determining the physical and chemical properties of supported metal particles [Valden et al., 1998; Hansen et al., 2002].

Apart from fundamental dynamic behaviors of metals on an oxide, metal-oxide interface properties are still poorly known in many respects despite long lasting efforts [Campbell, 1997]. This is due largely to difficulties in direct measurement/characterization of dynamic processes as well as buried interfaces at the atomic scale. Significant advances in computer power and theoretical methods over recent years have made it possible to explore metal particle dynamics and metal-dielectric interfacial interactions by using first principles quantum mechanics calculations [Verdozzi et al., 1999 Christensen and Carter, 2001; Siegel et al., 2002]. Such atomistic modeling in fact offers many valuable microscopic insights into those complex structural, dynamic, and electronic properties.

†To whom correspondence should be addressed.
E-mail: gshwang@che.utexas.edu
‡This paper is dedicated to Professor Hyun-Ku Rhee on the occasion of his retirement from Seoul National University.

In this paper we present the results of density functional theory (DFT) calculations on i) the geometric and electronic structures of stoichiometric and reduced TiO_2 (110) rutile surfaces and ii) the adsorption properties of Au, Ag, and Cu atoms on the TiO_2 (110) surfaces. Oxide supported Au, Ag and Cu nanometals often show markedly different physical and chemical characteristics. Recent experimental work [Boccuzzi et al., 2002], for instance, has shown that the Ag catalyst is almost inactive while Cu and Au catalysts exhibit intermediate and very high activities in the water gas shift reaction, respectively. The comparative study of oxide supported 1B metals is indeed a technologically and scientifically important subject.

The (110) rutile surface (which is the most thermodynamically stable among low-index TiO_2 surfaces) has been extensively studied both experimentally [Charlton et al., 1997; Diebold et al., 1996; Guo et al., 1996; Pang et al., 1998; Beennett et al., 1999] and theoretically [Bates et al., 1997; Lindan et al., 1997; Bredow and Pacchioni, 2002; Reinhardt and Hess, 1994; Ng and Vanderbilt, 1997]. However, a limited amount of theoretical work has been performed on the interaction of Au, Ag and Cu atoms with oxide surfaces. Moreover, there is no consensus in previous theoretical studies.

The adsorption properties of Au on stoichiometric TiO_2 (110) have been reported by several groups. Using the full potential linear muffin-tin orbital (FP-LMTO) calculations, Thiên-Nga and Paxton [1998] obtained a unreasonably large adsorption energy of 8.5 eV per Au atom on unrelaxed TiO_2(110). Using the full potential linearized augmented plane-wave method, Yang et al. [2000] estimated Au adsorption energies to be 1.0-1.49 eV per atom for three different adsorption sites. In these studies, the site atop a fivefold-coordinated Ti was predicted to be most favorable. On the other hand, based on planewave pseudopotential DFT-GGA slab calculation results, Lopez and Nørskov [2002] suggested that Au adsorbs preferably on a bridging O atom with the adsorption energy of 1.55 eV per atom. Contrary to these slab calculations, Giordano and his coworkers [Giordano et al., 2001] obtained small adsorption energies of less than 1 eV from their DFT-GGA cluster calculations. Their results also suggested the adsorption on top of a bridging O atom is most favorable. Using spin polarized DFT-GGA slab calculations, very recently, Vijay et al. [2003] and Wang and Hwang [2003] also reported very small Au adsorption energies of less than 0.61 eV on relaxed TiO_2 (110). However, both studies showed that the most stable adsorption site is atop the four-fold hollow position over the fivefold-coordinated Ti and in-plane and bridging O atoms, in which the covalent and ionic bonding interactions with the fivefold-coordinated Ti and the bridging O, respectively, contribute synergistically to the Au adsorption [Wang and Hwang, 2003].

While the calculation results are somewhat scattered, from fitting to experimental data using a kinetic model, the Au adsorption energy has been estimated to be as low as 0.43 eV on nearly stoichiometric TiO_2 (110) [Campbell et al., 2002].

The adsorption properties of Ag on stoichiometric TiO_2 (110) were studied by Giordano et al. [2001] using DFT-GGA cluster calculations. They obtained adsorption energies of 2.0 and 2.3 eV for the sites atop a bridging O atom and between two bridging O atoms, respectively. They also looked at the Cu adsorption properties which would be similar to the Ag adsorption with about 0.5 eV larger adsorption energies at the on-top and bridge sites.

Rutile TiO_2 (110) is likely to usually contain a significant number of oxygen vacancies [Onishi and Iwasawa, 1994; Murray et al., 1995; Schaub et al., 2003]. Recent theoretical studies have shown that the surface geometric and electronic structures of TiO_2 (110) are markedly altered by the presence of oxygen vacancies [Lindan et al., 1997; Bredow and Pacchioni, 2002]. The binding of Au to an oxygen vacancy site has been calculated to be substantially stronger than to the stoichiometric surface. For a 0.5 ML vacancy concentration on TiO_2 (110), Wahlström and his co-workers [Wahlström et al., 2003] obtained the Au adsorption energy of about 2.0 eV at the oxygen vacancy site by using planewave pseudopotential DFT-GGA slab calculations. For the same reduced surface, Vijay et al. [2003] and Wang and Hwang [2003] obtained the Au adsorption energy of about 2.3-2.5 eV using spin polarized DFT-GGA slab calculations. Wang and Hwang also showed there is a substantial reduction in the Au adsorption energy from 2.26 eV to 1.66 eV when the vacancy concentration is decreased from 0.5 ML to 0.33 ML (*vide infra*). For Ag and Cu adsorption on reduced TiO_2 (110), to our best knowledge, no theoretical study has been reported thus far.

COMPUTATIONAL DETAILS

Our quantum mechanics calculations are based on (spin-polarized) density functional theory (DFT) within the generalized gradient approximation (GGA) [Perdew et al., 1992], as implemented in the VASP code [Kresse and Hafner, 1993]. We also calculate the adsorption properties of Au and Ag on the stoichiometric TiO_2 (110) surface with the local spin density approximation (LSDA) with the Ceperly and Adler [1980] form parameterized by Perdew and Zunger [1981]. Mattson and Jennison [2002] recently showed that, due to weak metal interactions with the stoichiometric metal oxide surfaces, LDA was likely to provide better estimation in the metal/metal oxide binding relative to the GGA. We use Vanderbilt type ultrasoft pseudopotentials [Vanderbilt, 1990; Kresse and Hafner, 1994] and a plane-wave cutoff energy of 300 eV, which yields well-converged results. Charge densities are calculated by using the residual minimization method-direct inversion of the interactive subspace (RMM-DIIS) algorithm, and atomic structures are optimized by minimizing the Hellman-Feymann forces using the conjugate gradient method.

The oxide surfaces considered in this work are modeled by using a 15-atomic-layer slab that is separated from its vertical periodic image by a vacuum space of 10 Å, sufficient to describe the properties of the TiO_2 (110) surface (*vide infra*). All atoms are allowed to relax according to their atomic forces. For the Brillouin Zone integration, we use the lowest-order Monkhorst-Pack set of two k-points at (¼, ¼, 0) for the (1×1) surface cell, and one k point at (¼, ½, 0) for coverages of ½ for the geometry optimization. Total energies are evaluated by using a (4×6×1) mesh for the (1×1) surface cell, and (4×4×1) for larger surface cells.

RESULTS AND DISCUSSION

1. TiO_2 (110) Rutile Surfaces

Stoichiometric and reduced surfaces are depicted in Fig. 1. The TiO_2 structure, contains two types of Ti atoms and four different types of O atoms: five-fold coordinated Ti(5c), six-fold coordinated

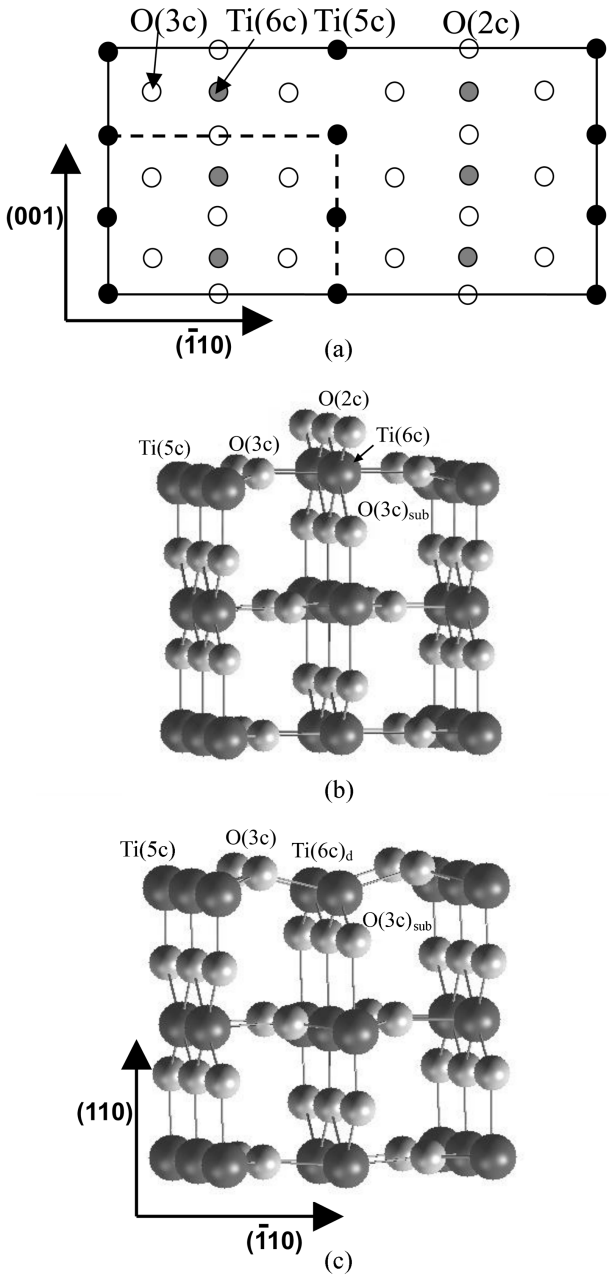

Fig. 1. Schematic representations of the TiO_2 (110) rutile surface. (a) 2×3 surface cell; the dotted line indicates the 1×2 surface cell. (b) side view of the stoichiometric surface. (c) side view of the reduced surface (with the row defect). The black and gray balls represent Ti and O atoms, respectively.

Ti(6c); two-fold coordinated bridging O(2c), three-fold coordinated in-plane O(3c), and two other subsurface O atoms. The reduced surfaces are created by removing the bridging O(2c) atoms. Oxygen vacancies are probably the most common surface defect on TiO_2 (110).

1-1. Stoichiometric Surface

Our GGA calculation results in the lattice constants of a=4.630 Å, c=2.979 Å and the internal parameter of u=0.305 (which indicates the location of oxygen atoms), and LDA results are: a=4.558 Å, c=2.925 Å and u=0.304, very close to the experimental results of a=4.594 Å, c=2.972 Å, and u=0.305 [Vinet et al., 1986].

In Table 1, we summarize the displacements of surface atoms, and compare them with other theoretical results [Bates et al., 1997] and experimental observations [Charlton et al., 1997]. The structural properties appear to be rather insensitive to the exchange and correlation functional [Muscat et al., 1999]. Our results are very close to the experimental values except the position of bridging O(2c) atoms (The O(2c) displacement of −0.04 Å is somewhat smaller than −0.27 Å as obtained from an X-ray spectroscopy measurement [Charlton et al., 1997], but it is in good agreement with other theoretical results [Bates et al., 1997]). This disagreement between theory and experiment may arise from the calculation method of nuclear positions in X-ray diffraction [Bates et al., 1997; Harrison et al., 1999]. The surface energy of 0.72-0.76 Jm^{-2} from our 15-atomic-layer slab model is virtually identical to 0.73 Jm^{-2} from a 21-atomic-layer slab model [Bates et al., 1997], indicating that a 15-atomic-layer slab is sufficient for describing the TiO_2 (110) surface.

1-2. Reduced Surfaces

Here, we consider i) completely and ii) partially reduced surfaces. The completely reduced surface is modeled by removing all bridging O(2c) atoms from the (2×1) surface cell. In fact, the formation of the completely reduced surface is unlikely [Bogicevic and Jennison, 2002]. However, it would be instructive to look at the difference between the completely and partially reduced surfaces.

For a partially reduced surface, a bridging O(2c) is removed from a given unit cell. In this study, to look at the vacancy-vacancy interaction, we employ several different sizes of surface cells which included (1×2), (1×3), (1×4), (1×5), (2×2), (2×3), and (2×4) unit cells.

When an bridging O(2c) is removed, neighboring atoms are displaced and the adjacent Ti(6c) atoms are reduced to Ti^{3+}. The atomic displacements of the reduced surface are summarized in Table 1. As expected, the adjacent Ti(6c), in-plane O(3c) and subsurface O atoms shift outward substantially.

For the different sizes of the surface cell, we calculate the oxygen vacancy formation energy, $E_f(V)$, which is defined as

Table 1. Atomic displacements of the TiO_2 rutile (110) surface

Atom	Stoichiometric (GGA)		From ref [23][a]		Exp. [18]		Reduced (GGA)	
	[110]	[−110]	[110]	[−110]	[110]	[−110]	[110]	[−110]
Ti(6c)	0.19	-	0.23	-	0.12±0.05	-	0.01	-
Ti(5c)	−0.15	-	−0.11	-	−0.16±0.05	-	−0.11	-
O(2c)	−0.02	-	−0.02	-	−0.27±0.08	-	-	-
O(3c)	0.18	0.06	0.18	0.05	0.05±0.05	0.16±0.08	0.44	0.09
$O(3c)_s$	−0.02	-	0.03	-	0.05±0.08	-	0.08	-

[a]The theoretical values were obtained using a 21-atomic layer slab model and a cutoff energy of 400 eV.

$$E_f(V) = E_{s-TiO2} - E_{r-TiO2} - E_O$$

where E_{s-TiO2}, E_{r-TiO2} and E_O are the total energies of the stoichiometric surface, the reduced surface, and a free O atom, respectively.

As listed in Table 2, the formation energy decreases significantly as the unit cell size is increased along the bridging O(2c) row from (1×2) to (1×5) and from (2×2) to (2×4). This result clearly demonstrates there exists a repulsive interaction between vacancies. We can also expect that the binding energy of adsorbates to the defect site is a strong function of the density and spatial distribution of vacancies. For a fully isolated neutral F_s center, however, it is expected that two excess electrons associated with the removed bridging O^{2-} are largely localized at the center of the vacancy due to the electrostatic stabilization by the inter-ionic Coulomb interactions of the ionic crystal [Ferrari and Pacchioni, 1995].

Table 2. Oxygen vacancy formation energy (in eV) calculated using different sizes of the surface unit cell, as indicated

	(1×2)	(1×3)	(1×4)	(1×5)	(2×2)	(2×3)	(2×4)
E_f (eV)	6.91	5.84	5.59	5.38	6.93	5.49	5.37

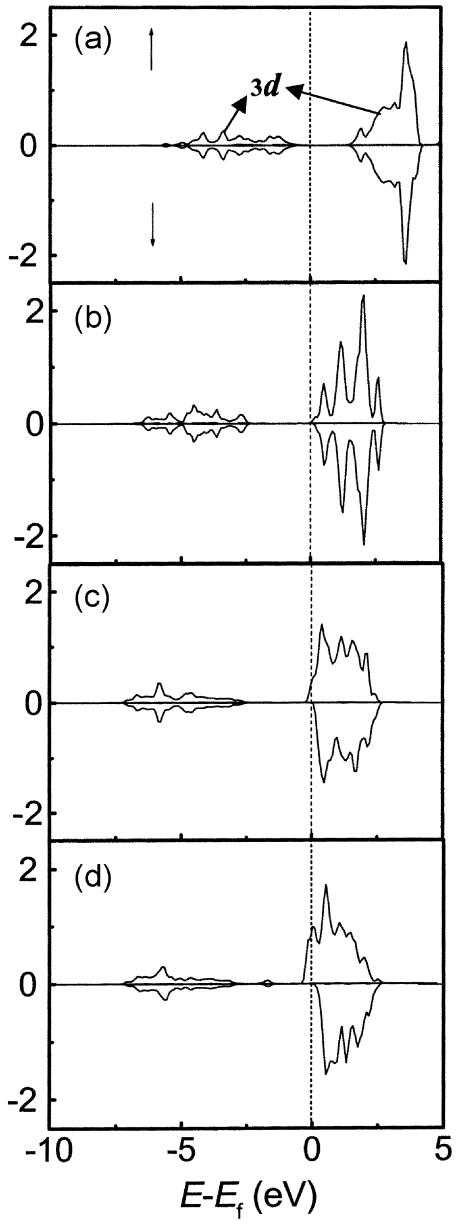

Fig. 2. LDOS for the spin-up (↑) and spin-down (↓) electrons of the Ti(6c) or [Ti(6c)$_d$] atom on (a) the stoichiometric surface and (b-d) reduced surfaces [(b) with a point defect (from the 1×3 surface cell), (c) with a point defect (from the 1×2 surface cell), (d) with the row defect (from the 1×2 surface cell)]. The dashed vertical line at E=0 eV indicates the Fermi level.

Fig. 2 shows the local density of states (LDOS) [Eichler et al., 1996] for the Ti(6c) atoms on the stoichiometric and reduced surfaces. For convenience, we roughly divide the energy into three different energy regimes: i) bonding area ($E-E_f \leq -4$ eV), ii) non-bonding area (-4 eV$<E-E_f<0$ eV), and iii) anti-bonding area ($E-E_f \geq 0$ eV). Compared to the stoichiometric surface [Fig. 2(a)], the vacancy defect causes the Ti 3d states to shift to the non-bonding area, indicating an increase in the reactivity of the defect site. The smaller (1×2) unit cell shows a broader distribution in the Ti 3d states, relative to the (1×3) case. More mixing of the Ti 3d states appears to occur

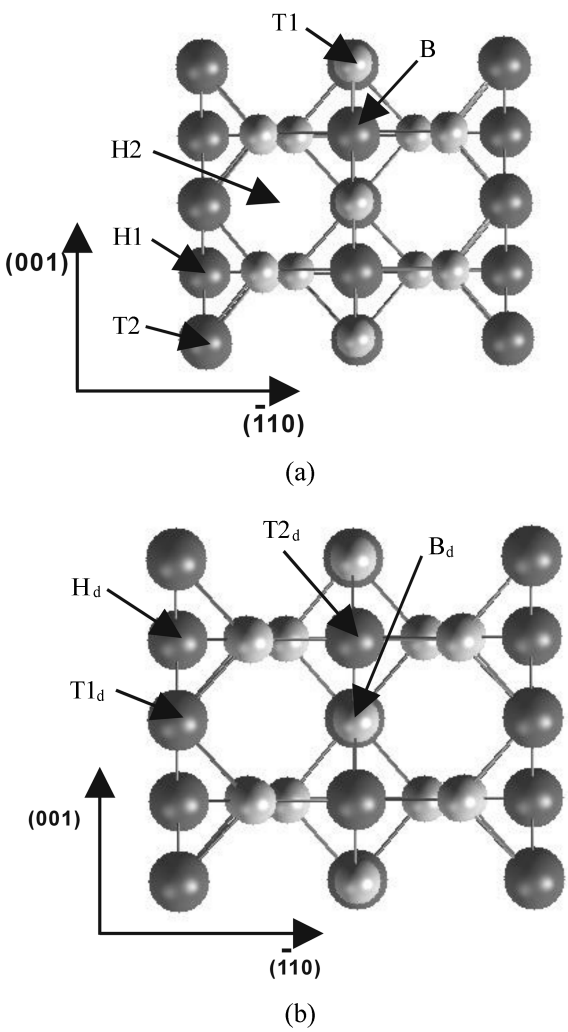

Fig. 3. Adsorption sites for (a) the stoichiometric surface and (b) the reduced surface. The black and gray balls represent Ti and O atoms, respectively.

in the completely reduced case. This suggests that the vacancies are delocalized, and interact strongly along a bridging O(2c) row. In addition, the 3d states shift to the non-bonding area when two vacancies are adjacent, for example in the (1×2) and completely reduced cases. This implies that a di-vacancy would be very unfavorable thermodynamically, which in turn results in a higher vacancy formation energy (or metal adsorption energies at the vacancy site).

2. Au, Ag and Cu Adsorption on TiO_2

For the Au, Ag and Cu adsorption on the stoichiometric TiO_2 (110) surface, as illustrated in Fig. 3(a), five different adsorption sites were considered: i) on top of a bridging O(2c) atom [indicated as T1], ii) on top of a fivefold coordinated Ti(5c) atom [T2], iii) between two bridging O(2c) atoms [B], iv) fourfold hollow over Ti(5c) and O(2c) atoms [H1], v) fourfold hollow over Ti(5c), O(2c), and O (3c) atoms [H2].

For the completely reduced TiO_2 (110) surface (which is modeled by removing bridging O(2c) atoms from the (1×2) surface unit cell), four different adsorption sites were considered [Fig. 3(b)]: i) fourfold hollow site over Ti(2) and O(2) atoms [indicated as H_d], ii) bridging two Ti(1) atoms [B_d], iii) on top of the Ti(2) atom [$T1_d$], and iv) on top Ti (1) atoms [$T2_d$]. However, we only considered the B_d site [which is the most favorable adsorption site (*vide infra*)] for partially reduced surfaces (which are modeled by removing a bridging oxygen atom from a given surface cell.

The adsorption energy (E_{ads}) of a metal atom (MA) on TiO_2 (110) is defined as

$$E_{ads}=E_{MA/TiO2}-E_{TiO2}-E_{MA}$$

where $E_{MA/TiO2}$, E_{TiO2}, E_{MA} are the total energies of the MA on the TiO_2 surface, the (stoichiometric or reduced) TiO_2 (110) surface, and a free metal atom, respectively. In addition, the interaction energy (E_{int}) between a metal atom and its periodic replicas for a given unit cell is also calculated as:

$$E_{ins}=E_{MA\_C}-E_{MA}$$

where E_{MA_C} is the total energy of a metal atom in a given unit cell (which includes a metal-metal interaction).

2-1. Au

2-1-1. On Stoichiometric TiO_2 (110)

The adsorption properties of Au on the stoichiometric TiO_2 (110) surface are summarized in Tables 3 and 4. A recent theoretical study [Wang and Hwang, 2003] suggests that, to avoid an interaction between adsorbed Au and its periodic replicas, the TiO_2 surface must be modeled using at least the (1×2) surface cell (in which the distance between the metal adatom and its periodic images is $d_{Au-Au}\geq 5.96$ Å).

For the (1×2) surface cell, we obtained the Au adsorption energies of 0.6 eV, 0.51 eV, 0.44 eV, 0.34 eV, and 0.33 eV per atom at the H2, T1, T2, H1, and B sites, respectively. According to this result, interestingly, the H2 site (which has been neglected in previous theoretical studies) turns out to be the most stable adsorption site. For the (1×2) supercell, the interaction between Au and its periodic replicas is insignificant (E_{int}=0.05 eV). The adsorption energy of 0.33-0.6 eV is very close to 0.43 eV as predicted by the Campbell group based on their experimental observations [Campbell et al., 2002]. For a comparison, our LDA values (in parentheses) are also listed in Table 3. The LDA-adsorption energies are far larger than the GGA energies (approximately twice), but the order in adsorption energy (for the different adsorption sites) remains unchanged.

Table 3. Adsorption properties of Au on stoichiometric TiO_2 (110) (from the 1×1 surface cell)

	H1	B	T1	T2	H2
E_{ad} (eV)	1.20	1.23	1.30	1.38	1.33
$d_{Au\text{-}Ti(5c)}$ (Å)	2.97	-	-	2.80	2.85
$d_{Au\text{-}O(2c)}$ (Å)	-	3.20	2.18	-	2.29
$d_{Au\text{-}O(3c)}$ (Å)	2.70	-	-	-	3.06

For the (1×1) unit cell, the Au-Au interaction is strong due to the short Au-Au distance of about 2.98 Å along the [001] direction. The calculated Au-Au interaction energy is $E_{int}\approx 1.21$ eV. The strong attractive Au-Au interaction results in a substantial reduction in the Au binding to the TiO_2 surface. (The Au adsorption energy decreases to 0.17 eV, 0.12 eV, 0.09 eV, 0.02 eV, and 0.0 eV at the T2, H2, T1, B, and H1 sites, respectively.) As a consequence, the Au-TiO_2 distance increases, e.g., at the T1 site, the Au-O(2c) distance increases from 2.3 Å to 3.2 Å. In the rather high coverage, the most favorable adsorption site appears to be on top of a Ti(5c) atom, which is consistent with previous DFT slab calculations [Lopez and Nørskov, 2002].

The sum of E_{ads} and E_{int} (at the most favorable site) increases by 0.73 eV as the unit cell size is changed from (1×2) to (1×1). The increase in the total energy is attributed to the Au-Au metallic interaction. Our calculated value of 1.38 eV for ($E_{ads}+E_{int}$) at the (1×1) unit cell is in good agreement with 1.04 eV from recent DFT-GGA (RPBE) slab calculations [Lopez and Nørskov, 2002].

2-1-2. On Reduced TiO_2 (110)

The adsorption properties of Au on the reduced TiO_2 (110) surfaces are summarized in Table 5. Here, we consider both partially and completely reduced surfaces. On the completely reduced surface, the Au adsorption energies are calculated to be 2.81 eV, 2.39 eV, 1.61 eV, and 1.48 eV at the B_d, T_{2d}, T_{1d}, and H_d sites, respectively, much larger than 0.3-0.6 eV on the stoichiometric surface. This suggests that the defect site [B_d], and the site atop an adjacent

Table 4. Adsorption properties of Au on stoichiometric TiO_2 (110) (from the 1×2 surface cell)

	H1	B	T1	T2	H2
E_{ad} (eV)	0.34 (0.92)	0.33 (0.98)	0.51 (0.98)	0.44 (0.92)	0.60 (1.25)
$d_{Au\text{-}Ti(5c)}$ (Å)	3.02 (2.83)	-	-	2.73 (2.57)	2.81 (2.67)
$d_{Au\text{-}O(2c)}$ (Å)	-	2.30 (2.30)	2.08 (2.01)	-	2.30 (2.18)
$d_{Au\text{-}O(3c)}$ (Å)	2.69 (2.53)	-	-	-	2.90 (2.83)

LDA values are shown in parentheses.

Table 5. Adsorption properties of Au on reduced TiO_2 (110)

	H_d[a]	$T1_d$[a]	$T2_d$[a]	B_d[a]	B_d[b]	B_d[c]	B_d[d]
E_{ad} (eV)	1.61	1.48	2.39	2.78	2.26	1.66	2.38
$d_{Au\text{-}Ti(6c)d}$ (Å)	-	-	2.51	2.69	2.63	2.64	2.65
$d_{Au\text{-}Ti(5c)}$ (Å)	2.77	2.50	-	-			
$d_{Au\text{-}O(3c)}$ (Å)	2.88	-	-	-			

[a]on the row defect (from the 1×2 surface cell)
[b]on the point defect (from the 1×2 surface cell)
[c]on the point defect (from the 1×3 surface cell)
[d]on the point defect (from the 2×2 surface cell)

Ti atom [T_{1d}] are far more stable than other sites considered for Au adsorption.

On a partially reduced surface, we only consider the B_d site (which is the most favorable Au adsorption site). Here, three different surface cells, (1×2), (1×3) and (2×2), are used to look at the defect density effect. The TiO_2 structure is affected weakly by vacancy density. However, as the surface cell size is increased from (1×2) to (1×3), the Au adsorption energy reduces significantly from 2.26 eV to 1.66 eV. Recall that the adsorption energy of 2.78 eV at the row defect is much higher than at the point defects. Like the vacancy formation energy, the Au adsorption energy also shows a strong dependence on the density of vacancies (along the bridging O(2c) row). The larger adsorption energy found for the smaller (1×2) cell is mainly attributed to the strong repulsive nature of vacancy-vacancy interactions, as discussed earlier. Looking at the energy difference between the (1×2) and (1×3) cells, 0.6 eV for the Au adsorption is almost a half of 1.2 eV for the vacancy formation. This implies that the defect site is not fully oxidized with Au; that is, the Au adsorbed defect sites still repel each other.

2-1-3. Electronic Structure and Bonding Mechanism

Au adsorption at the H2 site on the stoichiometric surface results in an insignificant change in the states of Ti(5c) and O(2c) surface atoms, which clearly demonstrates a weak interaction between the Au adatom and the TiO_2 surface. However, compared to metallic Au (100) [Fig. 4(a)], the Au 5d state is narrower and shifts substantially towards the Fermi energy level, and also the Au 6s state shifts closer to the Fermi energy (as a result of the reduction of wavefunction hybridization with neighboring atoms), as shown in Fig. 4(b). The large energy shift towards the Fermi energy level indicates a substantial increase in the chemical reactivity of the adsorbed Au atom [Hammer and Nrøskow, 1995]. The position of the d-state has been found to be a good measure of the reactivity for various systems.

For Au adsorbed at the B_d site on the reduced TiO_2 surface, as shown in Fig. 4(c), the Au 6s states appear below the Fermi energy level and the 5d states move to the bonding area and their width increases. This implies a strong interaction between the Au adatom and the reduced surface. In addition, the chemical reactivity of Au at F_s^0 is expected to be higher than that of the clean Au (100) surface.

Fig. 5 shows charge density differences (obtained by subtracting the superposition of a free Au atom and TiO_2 densities from the total density) for Au adsorption (a) over the O(2c) [T2], (b) over the Ti(5c) [T1], (c) over the four-fold hollow between O(2c) and Ti(5c) [H2]

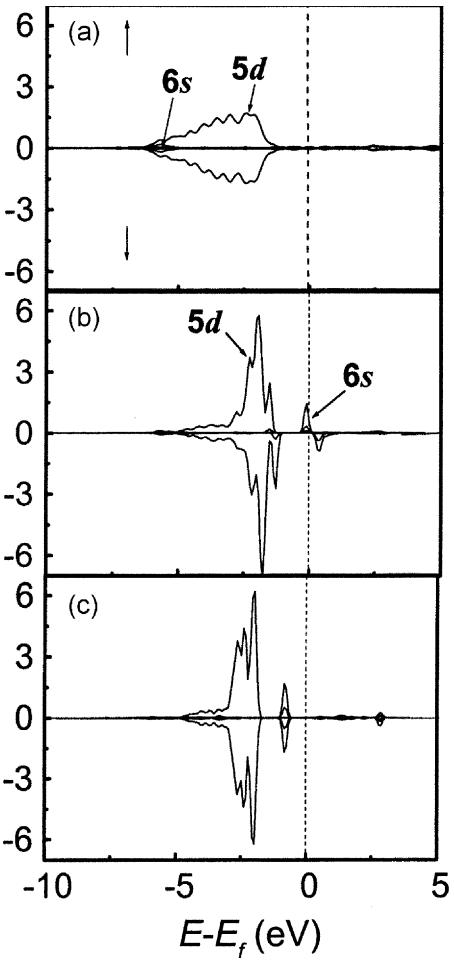

Fig. 4. LDOS for the spin-up (↑) and spin-down (↓) electrons of the Au atom. (a) metallic Au (100) surface atom. (b) Au adatom at the H2 site on the stoichiometric TiO_2 (110) surface. (c) Au adatom at the B_d site on the point defect site (from the 1×3 surface cell). The dashed vertical line at E= 0 eV indicates the Fermi level.

(from the (1×2) unit cell) on the stoichiometric surface, and (d) over the vacancy defect on a reduced surface. For T1 site adsorption [Fig. 5(a)], charge depletion between the adsorbed Au and the O(2c) is exhibited, along with some charge polarization of Au. On the other hand, as shown in Fig. 5(b), there is charge accumulation between the Au and the Ti(5c) atoms while the electron densities of both atoms appear reduce. From the Au adsorption energies of 0.51 eV (T1) and 0.44 eV (T2), we suspect that the magnitude of the Au interactions with the O(2c) and the Ti(5c) atom are comparable. For H2 site adsorption [Fig. 5(c)], it seems that electrons are repelled by the $O(2c)^{2-}$ anion and attracted by the $Ti(5c)^{4+}$ cation. The charge depletion of Au indicates there is some charge transfer from the Au adatom to the surface, presumably small considering the high ionization energy of Au. The density difference plots suggest that the adsorbed Au forms a weak covalent bond with the Ti(5c) and a weak ionic bond with the O(2c). At the H2 site, both the covalent and ionic interactions are likely to synergistically contribute to the Au adsorption, which can explain why the H2 adsorption site becomes energetically the most favorable.

For Au adsorption over a neutral F_s^0 center [Fig. 5(d)], there is

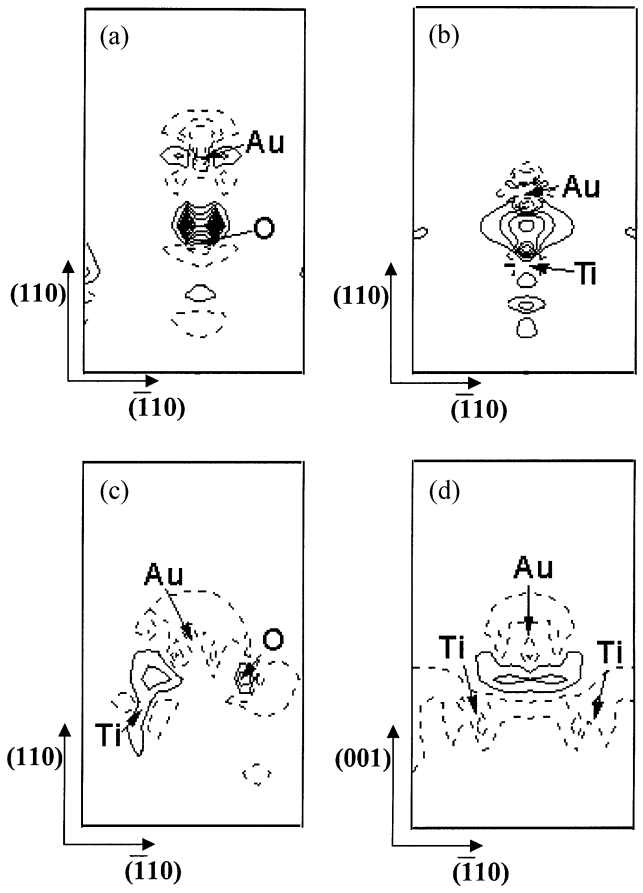

Fig. 5. Difference electron density plots (the total density is subtracted the superposition of atomic densities) for Au on TiO_2 (110) (a) at the T1 site, (b) at the T2 site, (c) at the H2 site, and (d) at the B_d site. The solid and dashed lines show positive and negative difference electron densities, respectively.

electron depletion in the reduced $Ti(6c)_d$ and electron accumulation in Au, implying some charge transfer from the Ti atoms to the Au atom. In addition, a significant polarization of Au towards the defect site is exhibited. This suggests an ionic interaction between the Au and the vacancy defect, like Ag on reduced MgO(100) in which one electron is likely to transfer from the F_s^0 center to the Ag atom to form an ionic Ag^--Fs^+ bond [Zhukovskii et al., 2000].

2-2. Ag

2-2-1. On Stoichiometric TiO_2 (110)

The adsorption properties of Ag on the stoichiometric TiO_2 (110) surface are summarized in Tables 6 and 7.

For the (1×2) surface cell, the most energetically favorable site for Ag adsorption is predicted to be the site between two bridging O(2c) atoms [B], with the adsorption energy of 1.01 eV, followed by T1 (0.81 eV), H2 (0.78 eV), T2 (0.37 eV), and H1 (0.32 eV) sites. A similar adsorption behavior was predicted by Giordano et al. [2001] using DFT-GGA cluster calculations, but their estimated adsorption energies of 0.34-2.30 eV substantially differ from our results. The interaction between Ag and its periodic replicas is estimated to be E_{int}=0.17 eV. This clearly demonstrates that a strong Ag-O(2c) interaction plays a major role in Ag adsorption.

Looking at Ag adsorption by using the (1×1) surface cell, the strong Ag-Ag interaction leads to significant reduction in the adsorption energy. The interaction between Ag and its periodic replicas is estimated to be E_{int}=1.17 eV, and the adsorption energies at the T2, H2, B, T1 sites, and H1 are 0.19 eV, 0.16 eV, 0.09 eV, 0.01 eV, and 0.01 eV, respectively. At the higher coverage, the most favorable adsorption site appears to be the T2 site, albeit the energy difference between different adsorption sites is very small.

Table 6. Adsorption properties of Ag on stoichiometric TiO_2 (110) (from the 1×2 surface unit cell)

	H1	B	T1	T2	H2
E_{ads} (eV)	0.32	1.01	0.81	0.37	0.78
$d_{AgTi(1)}$ (Å)	-	3.01	-	-	3.38
$d_{AgTi(2)}$ (Å)	3.13	-	-	2.86	3.18
$d_{AgO(1)}$ (Å)	-	2.22	2.12	-	2.17
$d_{AgO(2)}$ (Å)	2.70	-	-	-	2.77

Table 7. Adsorption properties of Ag on stoichiometric TiO_2 (110) (from the 1×1 surface unit cell)

	H1	B	T1	T2	H2
E_{ads} (eV)	0.01	0.09	0.19	0.01	0.16
$d_{AgTi(1)}$ (Å)	-	3.29	-	2.80	2.85
$d_{AgTi(2)}$ (Å)	3.38	-	-	-3.15	-
$d_{AgO(1)}$ (Å)	-	2.57	2.25	-	2.31
$d_{AgO(2)}$ (Å)	-	-	-	-	-

2-2-2. On Reduced TiO_2 (110)

Here, we only consider partially reduced surfaces modeled with the (1×2) and (1×3) surface cells.

The Ag adsorption energies at the B_d site are estimated to be 1.15 eV and 0.6 eV from the (1×2) and (1×3) surface cells, respectively. The significant difference is mainly attributed to the vacancy-vacancy repulsion on the reduced surface; that is, a larger repulsion in a smaller cell results in an increase in the calculated adsorption energy. Given that the vacancy-vacancy repulsive energy is greater than 0.47 eV on the (1×3) unit cell, (estimated from the vacancy formation energy difference between the (1×3) and (2×4) surface cells), one can expect that the Ag-defect interaction would be insignificant. This study clearly demonstrates that the Ag-defect interaction is much weaker than the Ag-O(2c) interaction on a typical TiO_2 (110) surface (with the defect coverage of lower than 10%). When Cu or Ag (with a singly occupied outer *s* orbital) is placed on the defect site, charge transferred from the defect site is likely to fill their antibonding states. This in turn causes the destabilization of the Cu or Ag adsorption on the defect site [Matveev et al., 1999]. In fact, a recent *ab initio* cluster calculation predicted the Ag-F_s interaction on MgO to be even repulsive [Ferrari and Pacchioni, 1995].

2-2-3. Electronic Structure and Bonding Mechanism

Fig. 6 shows the local density of states for (a) Ag (100), (b) Ag at the B site, and (c) Ag at the B_d site (from the (1×3) unit cell). The 4d state of Ag (100) is quite broad and exists at the bonding region, indicating the strong bonding interaction with neighboring Ag atoms. At the B site, the 4d state becomes narrower and the 5s state moves closer to the Fermi level. At the B_d site, the d-state position shifts noticeably towards the Fermi level and is even narrower than at the B site. The LDOS analysis confirms the weak interac-

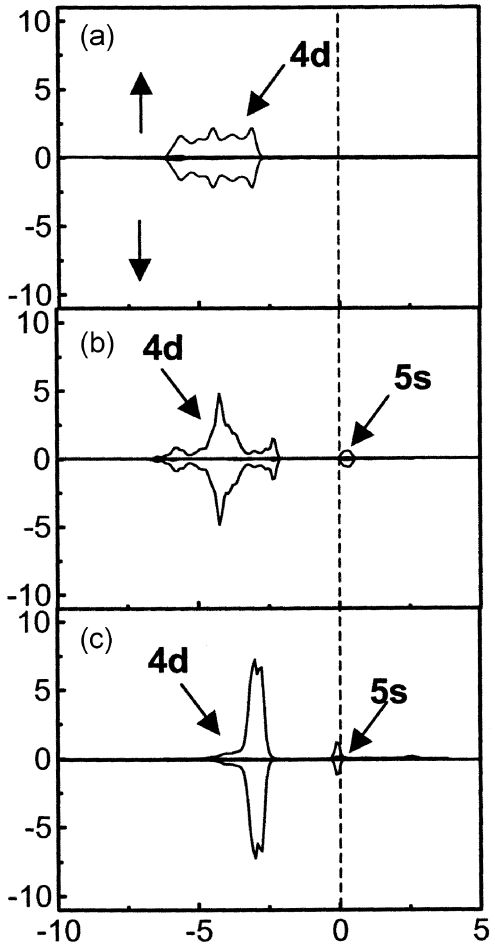

Fig. 6. LDOS for the spin-up (↑) and spin-down (↓) electrons of the Ag atom. (a) metallic Ag (100) surface atom. (b) Ag adatom at the B site on the stoichiometric TiO_2 (110) surface. (c) Ag adatom at the B_d site on the reduced surface (from the 1×3 surface cell). The dashed vertical line at E= 0 eV indicates the Fermi level.

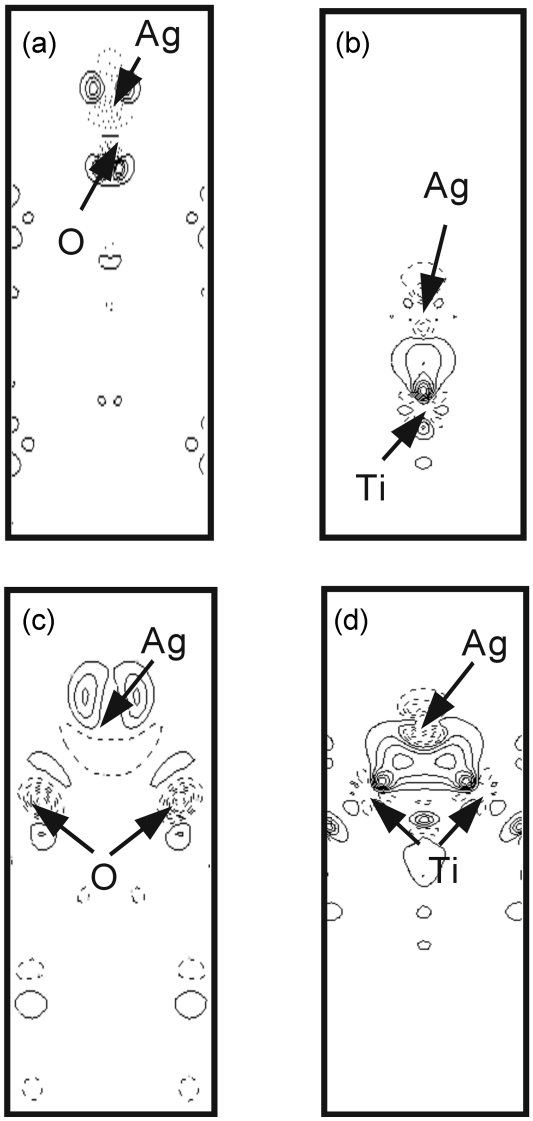

Fig. 7. Difference electron density plots (the total density is subtracted the superposition of atomic densities) for Ag on TiO_2 (110) (a) at the T1 site, (b) at the T2 site, (c) at the B site, and (d) at the B_d site. The solid and dashed lines show positive and negative difference electron densities, respectively.

tion of Ag with the defect site.

Fig. 7 shows charge density differences (obtained by subtracting the superposition of a free Ag atom and TiO_2 densities from the total density) for Ag adsorption (a) over the O(2c) [T1], (b) over the Ti(5c) [T2], (c) in between the two bridging O(2c)s [B] (from the (1×2) surface unit cell) on the stoichiometric surface, and (d) over the vacancy defect site (B_d) on the reduced surface (from the (1×3) unit cell). The charge density difference plots show that Ag binds to the Ti(5c) and the O(2c) via a covalent and ionic interaction, respectively. Unlike Au, the Ag-O(2c) electrostatic interaction appears to be approximately twice stronger than the Ag-Ti(5c) covalent interaction. When Ag is placed at the B site, the magnitude of the electrostatic attraction is likely to increase by interacting with two bridging O(2c) atoms. At the B_d site, there is charge accumulation in the region between Ag and reduced Ti atoms with some charge depletion in the metal atoms, suggesting the formation of covalent bonding.

2-3. Cu

2-3-1. On Stoichiometric TiO_2 (110)

The adsorption properties of Cu on stoichiometric TiO_2 (110) are summarized in Table 8. Like Ag, Cu strongly interacts with bridging O(2c) atoms, and Cu binds more strongly to the surface when it is placed closer to the O(2c) atoms. For the (1×2) surface cell, the most energetically favorable site for Cu adsorption is predicted to be the site between two bridging O(2c) atoms [B] with the adsorp-

Table 8. Adsorption properties of Cu on stoichiometric TiO_2 (110) (from the 1×2 surface unit cell)

	H1	B	T1	T2	H2
E_{ads} (eV)	0.79	1.80	1.43	0.56	1.61
$d_{Cu\text{-}Ti(1)}$ (Å)	2.72	-	-	-2.59	2.69
$d_{Cu\text{-}Ti(2)}$ (Å)	-	2.63	-	-	2.91
$d_{Cu\text{-}O(1)}$ (Å)	2.07	-	-	-	2.16
$d_{Cu\text{-}O(2)}$ (Å)	-	1.85	1.82-	-	1.92

tion energy of 1.80 eV, followed by T1 (1.61 eV), H2 (1.43 eV), H1 (0.79 eV), and T2 (0.56 eV) sites. The adsorption energies are in good agreement with 0.50-2.67 eV and 0.55-2.39 eV as obtained by Giordano et al. [2001] using cluster and slab calculations, respectively. We also calculated a change in the adsorption energy by varying the slab thickness from 15- to 21-atomic layers. We found that the adsorption energy changes by only about 0.1 eV at the B site. This suggests that the 15 layer slab is sufficient to look at Cu adsorption properties. For the (1×2) surface cell, the interaction between Cu and its periodic replicas is E_{int}=0.24 eV.

Our calculation results demonstrate the interaction of Cu with TiO_2 (110) is stronger, compared to Au and Ag. Unlike Au and Ag, even at a higher coverage (from the (1×1) cell), Cu binds strongly to the surface with the adsorption energy of around 0.8 eV at the B site (for instance). This is consistent with an experimental observation of the self limiting growth of Cu particles (i.e., the particle size remains constant and only the particle density increases with an increase in deposition [Zhou et al., 2003]). Au and Ag particles, on the other hand, experience Ostwald ripening during the growth.

2-3-2. On Reduced TiO_2 (110)

The adsorption energy of a Cu atom at the B_d site is 1.0 eV (from a (1×3) unit cell). This adsorption energy is significantly lower than the stoichiometric surface, which was also observed for Ag.

2-3-3. Electronic Structure and Bonding Mechanism

Fig. 8 shows the local density of states for (a) Cu(100), (b) Cu at the B site, and (c) Cu at the B_d site (from the (1×3) unit cell). Overall, compared to the Au and Ag d states, the Cu 3d states exist closer to the Fermi level, indicating that the Cu activity is greater than Au and Ag activity, consistent with experimental observations.

Fig. 9 shows charge density differences (obtained by subtracting the superposition of a free Cu atom and TiO_2 densities from the total density) for Cu adsorption (a) over the O(2c) [T1], (b) over the Ti(5c) [T2], (c) in between the two bridging O(2c)s [B] (from the (1×2) surface unit cell) on the stoichiometric surface, and (d) over the vacancy defect site (B_d) on the reduced surface (from the (1×3) unit cell). The Cu-surface bonding mechanism is similar to the Ag-sur-

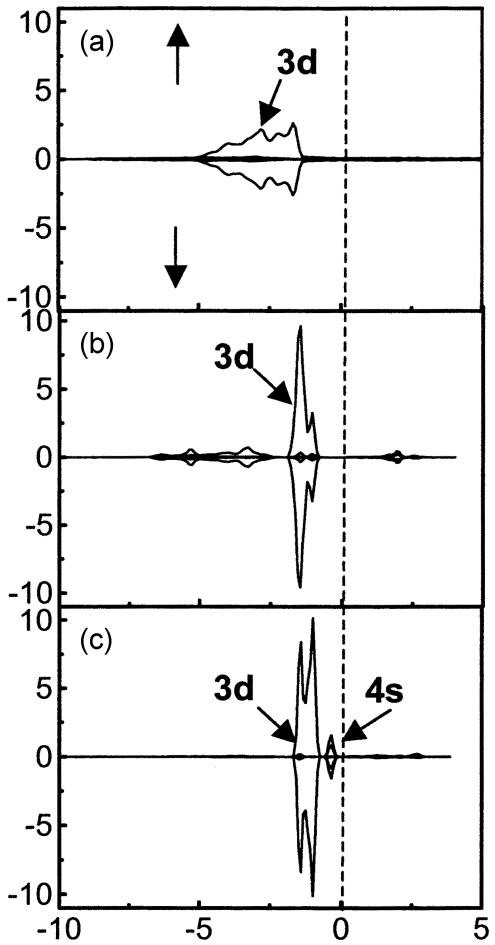

Fig. 8. LDOS for the spin-up (↑) and spin-down (↓) electrons of the Cu atom. (a) metallic Cu (100) surface atom. (b) Cu adatom at the B site on the stoichiometric TiO_2 (110) surface. (c) Cu adatom at the B_d site on the reduced surface (from the 1×3 surface cell). The dashed vertical line at E= 0 eV indicates the Fermi level.

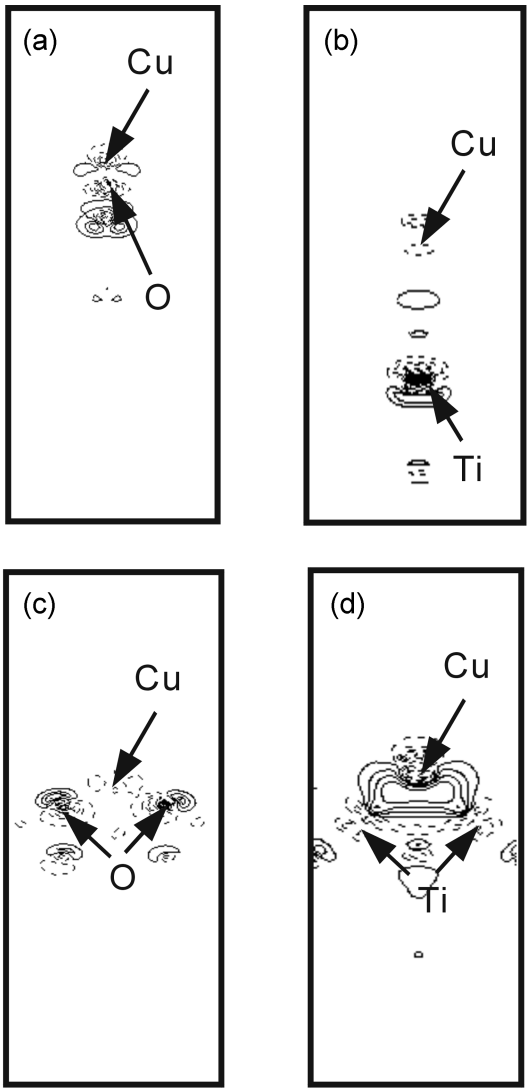

Fig. 9. Difference electron density plots (the total density is subtracted the superposition of atomic densities) for Cu on TiO_2 (110) (a) at the T1 site, (b) at the T2 site, (c) at the B site, and (d) at the B_d site. The solid and dashed lines show positive and negative difference electron densities, respectively.

face system. Fig. 9(d) shows that the binding of Cu to the defect site is mainly by the covalent interaction with $Ti(6c)_d$ atoms.

SUMMARY

We report the results of density functional theory slab calculations on (1) the geometric and electronic structures of stoichiometric and reduced TiO_2 (110) rutile surfaces, and (2) the adsorption of Au, Ag, and Cu atoms on the rutile surfaces. In this work, we attempted to (1) address a change in the surface properties of TiO_2 (110) with oxygen vacancy defects and a vacancy-vacancy interaction on the reduced surfaces, (2) identify the preferred adsorption sites of Au, Ag, and Cu atoms on the stoichiometric and reduced surfaces and their bonding mechanisms, and (3) develop the general trend in the adsorption properties and electronic structures of TiO_2 supported 1B metals as one goes from Au, Ag to Cu.

We consider not only partially reduced but also completely reduced TiO_2 surfaces for the purpose of instructions (although the latter is very unlikely in reality). Oxygen vacancies result in significant changes in the position of five-coordinated Ti(5c) and inplane O(3c) surface atoms and the position of reduced $Ti(6c)_d$ 3d states and O(3c) 2s states. The vacancy formation turns out to be a strong function of the density of vacancies (particularly along the bridging oxygen row.). Increased mixing of the $Ti(6c)_d$ 3d states appears to occur when two vacancies stay nearby, suggesting that the vacancies are delocalized and interact each other strongly. Our study suggests that the vacancies prefer to be widely distributed, rather than forming clusters.

For Au adsorption on the stoichiometric surface, we find that the H2 site [fourfold hollow over the in-plane O(3c), the Ti(5c) and the bridging O(2c)] is energetically the most stable site, with an adsorption energy of ≈0.6 eV. Charge density difference plots suggest that the adsorbed Au shows a covalent interaction with Ti(5c) and an ionic interaction with the O(2c). It turns out that the covalent and ionic interactions are comparable in magnitude. At the H2 site, both the covalent and ionic interactions contribute synergistically to Au adsorption. For Au on top of the vacancy site, charge transfer occurs from the defect site to the adsorbed Au, suggesting ionic bond formation between the adsorbed Au and surrounding $Ti(6c)_d$ atoms. According to our DFT-GGA results, the binding of Au to the defect site is far stronger than on the stoichiometric surface. This suggests that vacancy sites could serve as nucleation centers for Au particles.

Ag and Cu atoms strongly interact with the bridging O(2c) of the surface. Therefore, the B site [in between two bridging O(2c) atoms] is the most favorable energetically. The adsorption energies of Ag and Cu at the B site are estimated to be 1.01 eV and 1.80 eV, respectively, from the (1×2) surface cell. Ag and Cu atoms also covalently interact with the surface Ti(5c), but their interaction of about E_{ads}≈0.6 eV is far weaker than the Ag/Cu-O(2c) interaction of E_{ads}≈ 1.0/1.6 eV. Unlike Au, the interaction of Ag and Cu with a vacancy site is much weaker than with the stoichiometric surface. When a metal atom is placed on the vacancy site, generally some charge is transferred from the defect to the metal, which subsequently leads to the formation of a strong ionic metal-defect bond. However, for Cu or Ag (with a singly occupied outer s orbital), the transferred charge is likely to fill the antibonding states of Ag and Cu and thus destabilize the Cu or Ag adsorption. Our charge density difference plots demonstrate the binding of Ag and Cu to the surface is attributed mainly to covalent bonding with $Ti(6c)_d$ atoms.

ACKNOWLEDGMENT

The authors acknowledge the Welch Foundation (Grant No. F-1535) for their financial support of this work.

REFERENCES

Bates, S. P., Kresse, G. and Gillan, M. J., "A Systematic Study of the Surface Energetics and Structure of TiO_2 (110) by First-principles Calculations," *Surf. Sci.*, **385**, 386 (1997).

Bell, A. T., "The Impact of Nanoscience on Heterogeneous Catalysis," *Science*, **299**, 1688 (2003).

Bennett, R. A., Stone, P., Price, N. J. and Bowker, M., "Two (1×2) Reconstructions of TiO_2 (110): Surface Rearrangement and Reactivity Studied using Elevated Temperature Scanning Tunneling Microscopy," *Phys. Rev. Lett.*, **82**, 3831 (1999).

Boccuzzi, F., Chiorino, A., Manzoli, M., Andreeva, D., Tabakova, T., Ilieva, L. and Iadakiev, V., "Cold, Silver and Copper Catalysts Supported onTiO_2 for Pure Hydrogen Production," *Catal. Today*, **75**, 169 (2002).

Bogicevic, A. and Jennison, D. R., "Effect of Oxide Vacancies on Metal Island Nucleation," *Surf. Sci.*, **515**, L481-L486 (2002).

Bredow, T. and Pacchioni, G., "Electronic Structure of an Isolated Oxygen Vacancy at the TiO_2 (110) Surface," *Chem. Phys. Lett.*, **355**, 417 (2002).

Campbell, C. T., Parker, S. C. and Starr, D. E., "The Effect of Size-Dependent Nanoparticle Energetics on Catalyst Sintering," *Science*, **298**, 811 (2002).

Campbell, C. T., "Ultrathin Metal Films and Particles on Oxide Surfaces: Structural, Electronic and Chemisorptive Properties," *Surf. Sci. Rep.*, **27**, 1 (1997).

Ceperley, D. M. and Alder, B. J., "Ground-state of the Electron Gas by a Stochastic Method," *Phys. Rev. Lett.*, **45**, 566 (1980).

Charlton, G., Howes, P., Nicklin, C., Steadman, P., Taylor, J., Muryn, C., Harte, S., Mercer, J., McGrath, R., Norman, D., Turner, T. and Thornton, G., "Relaxation of TiO_2(110)-(1×1) using Surface X-ray Diffraction," *Phys. Rev. Lett.*, **78**, 495 (1997).

Choudhary, T. V. and Goodman, D. W., "Oxidation Catalyst by Supported Gold Nano-clusters," *Top. Catal.*, **21**, 1 (2002).

Christensen, A. and Carter, E. A., "Adhesion of Ultrathin ZrO_2(111) Films on Ni(111) from First Principles," *J. Chem. Phys.*, **114**, 5816 (2001).

de Oliveira, A. L., Wolf, A. and Schuta, F., "Highly Selective Propene Epoxidation with Hydrogen/oxygen Mixtures over Titania-supported Silver Catalysts," *Catal. Lett.*, **73**, 157 (2001).

Diebold, U., Anderson, J. F., Ng, K.-O. and Vanderbilt, D., "Evidence for the Tunneling Site on Transition-metal Oxides: TiO_2 (110)," *Phys. Rev. Lett.*, **77**, 1322 (1996).

Eichler, A., Hafner, J., Furthmüller, J. and Kresse, G., "Structural and Electronic Properties of Rhodium Surfaces: An ab initio Approach," *Surf. Sci.*, **346**, 300 (1996).

Ferrari, A. M. and Pacchioni, G., "Electronic Structure of F and V Centers on the MgO Surface," *J. Phys. Chem.*, **99**, 17010 (1995).

Giordano, L., Pacchioni, G., Bredow, T. and Sanz, J. F., "Cu, Ag, and Au Atoms Adsorbed on TiO_2 (110): Cluster and Periodic Calculations," *Surf. Sci*., **471**, 21 (2001).

Guo, Q., Cocks, I. and Williams, E. M., "Surface Structure of (1×2) Reconstructed TiO_2 (110) Studied using Electron Stimulated Desorption ion Angular Distribution," *Phys. Rev. Lett*., **77**, 3851 (1996).

Hammer, B. and Nørskov, J. K., "Electronic Factors Determining the Reactivity of Metal Surfaces," *Surf. Sci*., **343**, 211 (1995).

Hansen, P. L., Wagner, J. B., Helveg, S., Rostrup-Nielsen, J. R., Clausen, B. S. and Topsoe, H., "Atom-Resolved Imaging of Dynamic Shape Changes in Supported Copper Nanocrystals," *Science*, **295**, 2053 (2002).

Harrison, N. M., Wang, X. G., Muscat, J. and Scheffler, M., "The Influence of Soft Vibrational Modes on our Understanding of Oxide Surface Structure," *Faraday Discussions*, **114**, 305 (1999).

Haruta, M., "Size- and Support-dependency in the Catalysis of Gold," *Catal. Today*, **36**, 153 (1997).

Hayash, T., Tanaka, K. and Haruta, M., "Selective Vapor-phase Epoxidation of Propylene over Au/TiO_2 Catalysts in the Presence of Oxygen and Hydrogen," *J. Catal*., **178**, 566 (1998).

Kolmakov, A. and Goodman, D. W., "Imaging Gold Clusters on TiO_2 (110) at Elevated Pressures and Temperatures," *Catal. Lett*., **70**, 93 (2000).

Kolmakov, A. and Goodman, D. W., "Scanning Tunneling Microscopy of Gold Clusters on TiO_2 (110): CO Oxidation at Elevated Pressures," *Surf. Sci*., **490**, L 597-L601 (2001).

Kresse, G. and Hafner, J., " Ab-initio Molecular-dynamics for Liquid-metals," *Phys. Rev. B*, **47**, RC558 (1993); Kresse, G. and Furthmüller, J., "Efficient Iterative Schemes for ab initio Total-energy Calculations using a Plane-wave Basis Set," *Phys. Rev. B*, **54**, 11169 (1996).

Kresse, G. and Hafner, J., "Norm-conserving and Ultra-soft Pseudopotentials First-row and Transition Elements," *J. Phys.*: *Condens. Matter*, **6**, 8245 (1994).

Lindan, P. J. D., Harrison, N. M., Gillan, M. J. and White, J. A., "First-principles Spin-polarized Calculations on the Reduced and Reconstructed TiO_2 (110) Surface," *Phys. Rev. B*, **55**, 15919 (1997).

Lopez, N. and Nørskov, J. K., "Theoretical Study of the Au/TiO_2 (110) Interface," *Surf. Sci.*, **515**, 175 (2002).

Mattsson, A. E. and Jennison, D. R., "Computing Accurate Surface Energies and the Importance of Electron Self-energy in Metal/metal-oxide Adhesion," *Surf. Sci*., **520**, L611-L618 (2002).

Matveev, A. V., Neyman, K. M., Yudanov, I. V. and Rosch, N., "Adsorption of Transition Metal Atoms on Oxygen Vacancies and Regular Sites of the MgO(001) Surface," *Surf. Sci*., **426**, 123 (1999)].

Murray, P. W., Condon, N. G. and Thornton, G., "Effect of Stoichiometry on the Structure of TiO_2 (110)," *Phys. Rev. B*, **51**, 10989 (1995).

Muscat, J., Harrison, N. M. and Thorton, G., "First-principles Study of Potassium Adsorption on TiO_2 Surfaces," *Phys. Rev. B*, **59**, 2320 (1999).

Ng, K.-O. and Vanderbilt, D., "Structure and Apparent Topography of TiO_2 (110) Surfaces," *Phys. Rev. B*, **56**, 10544 (1997).

Onishi, H. and Iwasawa, Y., "Reconstruction of TiO_2 (110) Surface - STM Study with Atomic Scale Resolution," *Surf. Sci*., **313**, L783-L789 (1994).

Pang, C. L., Haycock, S. A., Raza, H., Murray, P. W., Thornton, G., Gulesren, O., James, R. and Bullett, D. W., "Added Row Model of TiO_2 (110) 1×2," *Phys. Rev. B*, **58**, 1586 (1998).

Perdew, J. and Zunger, A., "Self Interaction Correction to Density-functional Approximations for Many-electron Systems," *Phys. Rev. B*, **23**, 5048 (1981).

Perdew, J., Chevary, J., Vosko, S., Jackson, K., Pederson, M., Singh, D. and Fiolhais, C., "Atoms, Molecules, Solids, and Surfaces - Applications of the Generalized Gradient Approximation for Exchange and Correlation," *Phys. Rev. B*, **46**, 6671 (1992).

Reinhardt, P. and Hess, B. A., "Electronic and Geometrical Structure of Rutile Surfaces," *Phys. Rev. B*, **50**, 12015 (1994).

Santra, A. K. and Goodman, D. W., "Oxide-supported Metal Clusters: Models for Heterogeneous Catalysts," *J. Phys.: Condens. Matter*, **14**, R31-R62 (2002).

Schaub, R., Wahlström, E., Rønnau, A., Lægsgaard, E., Stensgaad, I. and Besenbacher, F., "Oxygen-mediated Diffusion of Oxygen Vacancies on the TiO_2 (110) Surface," *Science*, **299**, 377 (2003).

Siegel, D. J., Hector, L. G. and Adams, J. B., "Adhesion, Atomic Structure, and Bonding at the Al (111)/α-Al_2O_3 (0001) Interface: A First Principles Study," *Phys. Rev. B*, **65**, 85415 (2002).

Thiên-Nga, L. and Paxon, A. T., "Electronic Structure of 5d Transition Metals Adsorbed on the Stoichiometric (110) Rutile Surface," *Phys. Rev. B*, **58**, 13233 (1998).

Valden, M., Lai, X. and Goodman, D. W., "Onset of Catalytic Activity of Gold Clusters on Titania with the Appearance of Nonmetallic Properties," *Science*, **281**, 1647 (1998).

Vanderbilt, D., "Soft Slef-consistent Pseudopotentials in a Generalized Eigenvalue Formalism," *Phys. Rev. B*, **41**, 7892 (1990).

Verdozzi, C., Jennison, D. R., Schultz, P. A. and Sears, M. P., "Sapphire (0001) Surface, Clean and with d-Metal Overlayers," *Phys. Rev. Lett*., **82**, 799 (1999).

Vijay, A., Mills, G. and Meitu, H., "Adsorption of Gold on Stoichiometric and Reduced Rutile TiO_2 (110) Surfaces," *J. Chem. Phys*., **118**, 6536 (2003).

Vinet, P., Ferrante, J., Smith, J. R. and Hose, J. H., "A Universal Equation of State for Solids," *J. Phys.: Condens. Matter*, **19**, L467-L473 (1986).

Wahlström, E., Lopez, N., Schaub, R., Thostrup, P., Rønnau, A., Africh, C., Lægsgaard, E., Nørskov, J. K. and Besenbacher, F., "Bonding of Gold Nanoclusters o Oxygen Vacancies on Rutile TiO_2 (110)," *Phys. Rev. Lett*., **90**, 26101 (2003).

Wang, Y. and Hwang, G. S., "Adsorption of Au Atoms on Stoichiometric and Reduced TiO_2 (110) Rutile Surfaces: A First Principles Study," *Surf. Sci*., **542**, 72 (2003).

Yang, Z., Wu, R. and Goodman, D. W., "First-principles Study of the Adsorption of CO on TiO_2(110)," *Phys. Rev. B*, **61**, 14066 (2000).

Zhou, J., Kang, Y. C. and Chen, D. A., "Controlling Island Size Distributions: A Comparison of Nickel and Copper Growth on TiO_2 (110)," *Surf. Sci*., **537**, L429-L434 (2003).

Zhukovskii, Y. F., Kotomin, E. A., Jacobs, P. W. M. and Stoneham, A. M., "Ab Initio Modeling of Metal Adhesion on Oxide Surfaces with Defects," *Phys. Rev. Lett*., **84**, 1256 (2000).

"Electronic Factors Determining the Reactivity of Metal Surfaces," *Surf. Sci*., **343**, 211 (1995).